

Hydrogen storage properties of rare earth (RE) borohydrides

(RE = La, Er) in composite mixtures with LiBH_4 and LiH .

Christoph Frommen^a, Michael Heere^a, Marit D. Riktor^{a,b}, Magnus H. Sørby^a, Bjørn C. Hauback^{a,*}

^aInstitute for Energy Technology, Physics Department, P.O. Box 40, NO-2027 Kjeller, Norway

^bSINTEF Materials and Chemistry, Forskningsveien 1, NO-0314 Oslo, Norway

Keywords: borohydride, rare earth, hydrogen storage, composite

Abstract

Mixtures of $6\text{LiBH}_4\text{-RECl}_3\text{-3LiH}$ (RE=La, Er) have been produced by mechanochemical milling and their structure, thermal decomposition and reversibility have been studied. Hydrogen desorption starts around 300 °C in both composites. Heating to 400 °C yields LaB_6 , ErB_4 and $\text{REH}_{2+\delta}$ as major decomposition products. LiBH_4 is destabilized by $\text{REH}_{2+\delta}$ formed through decomposition of the parent borohydrides $\text{LiLa}(\text{BH}_4)_3\text{Cl}$ and $\text{Er}(\text{BH}_4)_3$, respectively, and its hydrogen release temperature is reduced by 100 °C as compared to pure ball-milled LiBH_4 . The lanthanum-containing composite releases 4.2wt% H between 300 and 350 °C and shows a limited reversibility of ~20% (340 °C, 10 MPa) probably due to hydrogen uptake by some amorphous boron-containing phases. For $6\text{LiBH}_4\text{-ErCl}_3\text{-3LiH}$ about 3wt% H is evolved up to 400 °C. Desorption against 0.5 MPa backpressure results in an increased reversibility (~80

* Corresponding author
Phone: +47 97 40 88 44
Email: bjorn.hauback@ife.no

%) as compared to vacuum (~66 %). Rehydrogenation (340 °C, 10 MPa) shows the formation of ErH₃ and LiBH₄ at drastically reduced conditions compared to pure LiBH₄ (>400 °C, >10 MPa).

Introduction

Rare earth (RE) borohydrides have received considerable attention during the past 5 years due to their rich crystal chemistry [1-7] and potential as both solid state hydrogen storage materials [8-15] and solid state electrolytes [16-18]. Special interest has been directed lately towards the development of easy and facile synthesis routes for solvent-free borohydrides [19-21]. Mechanochemical synthesis that utilizes a metathesis reaction between a RE-chloride and an alkali metal borohydride (mostly LiBH₄) is now the standard technique for the synthesis of RE-borohydrides. We have recently reviewed the crystal chemistry and thermal properties of ball-milled mixtures between RECl₃ and LiBH₄ [2]. We observe the formation of a series of RE-borohydrides with four distinct structure types which are determined by the ionic radius of the RE and its electronic configuration. The early lanthanides La, Ce, Pr, and Nd form LiRE(BH₄)₃Cl compounds (cubic; *I-43m*), Sm, Gd, Tb, Er and Yb form α -RE(BH₄)₃ (cubic; *P α -3*) with a possible polymorphic transition to β -RE(BH₄)₃ for Y, Yb (cubic; *P β -3m* or *F β -3m*) [1-3, 5-7, 11, 16, 17]. The smallest lanthanides Yb and Lu form tetrahedral [RE(BH₄)₄]⁻ anionic complexes that are stabilized by Li⁺ cations (tetragonal; *P-42c*) in analogy to LiSc(BH₄)₄ [22]. Furthermore, Sm and Gd show transitions to the LiRE(BH₄)₃Cl structure type that is observed for the largest lanthanide ions [17].

The RE-borohydrides obtained by mechanochemical synthesis decompose between 200 and 300 °C [5, 6, 11, 12, 16, 17], which is considerably lower than pure LiBH₄ [23]. With the exception of Yb-based compounds [3], they release primarily hydrogen and form RE-hydrides and borides as the major decomposition products. Gennari et al. have recently reported the destabilization of LiBH₄ via the formation of RE-hydrides in 6LiBH₄-RECl₃ composites (RE= Ce, Gd) [13]. We have extended this study to a

wide range of novel RE borohydrides [2]. Here, we present new experimental results based on *ex-situ* powder X-ray diffraction (PXRD), thermogravimetric and caloric measurements (TG/DSC), and cycling experiments for La- and Er-based borohydrides in composite mixtures with LiBH_4 and LiH. We elucidate the nature of products formed during different experimental conditions, e.g. decomposition under back pressure and vacuum. Finally, we compare the hydrogen storage properties and benchmark the reversibility of the La- and Er-based composites against previously investigated $6\text{LiBH}_4\text{-RECl}_3\text{-3LiH}$ systems (RE=Ce, Gd).

Experimental

Sample Preparation: LiBH_4 (Sigma-Aldrich, >95%), LaCl_3 and ErCl_3 (both Sigma-Aldrich, > 99.99%) in a 6:1 ratio were first milled in a Fritsch Pulverisette 6 at 400 rpm with a milling time of 5 hours. In the second step, LiH (Sigma-Aldrich >95%) was added (molar ratio LiH:RE = 3) and milled for an additional hour. Stainless steel vial and balls were used and a ball-to-powder ratio of 40:1 was applied. All sample handling was performed under strictly inert conditions and samples were stored in an MBraun glove box fitted with recirculation system and oxygen/humidity sensors. Oxygen and water levels were kept below 1 ppm during all operations.

PXD: Patterns were collected in transmission mode using Cu-K_α radiation (1.5418 Å) in a Bruker AXS D8 Advance diffractometer equipped with a Göbel mirror and LynxEye™ 1D strip detector. In addition, Synchrotron Radiation (SR) PXD patterns with a wavelength of 0.50513 Å were recorded at the Swiss-Norwegian Beam Line (SNBL, BM01B) at ESRF, Grenoble, in France. Data were collected with a DEXEL Perkin Elmer 2923 CMOS pixel detector. All samples were contained in rotating boron glass capillaries (0.5 mm diameter) filled and sealed under Ar atmosphere.

TG/DSC: Simultaneous TG/DSC experiments were conducted under flowing Argon gas (flow: 50 ml/min) in a Netzsch STA 449 F3 Jupiter instrument between room temperature (RT) and 400 °C with a heating rate of 2 °C/min. Samples were contained in Al crucibles fitted with pierced lids. The data were baseline corrected using two empty Al pans in the reference and sample position which were heated under identical conditions. The desorbed gases were analyzed with a MKS Microvision-IP residual gas analyzer (RGA) by mass spectroscopy (MS).

Dehydrogenation and rehydrogenation: The $6\text{LiBH}_4\text{-RECl}_3$ and $6\text{LiBH}_4\text{-RECl}_3\text{-3LiH}$ (RE=La, Er) composite mixtures were cycled in a Sieverts apparatus that was built in-house. Decomposition was either performed under vacuum or against 0.5 MPa backpressure at 400 °C for 12 hours. Rehydrogenation was performed at 340 °C under 10 MPa hydrogen pressure for 12 hours.

Results

$6\text{LiBH}_4\text{-LaCl}_3\text{-3LiH}$: The PXD pattern of as-milled $6\text{LiBH}_4\text{-LaCl}_3\text{-3LiH}$ in Fig. 1 shows the presence of three major crystalline phases: LiCl, LiBH_4 , and LiH, and their peak positions have been indicated by tick marks. Crystalline $\text{LiLa}(\text{BH}_4)_3\text{Cl}$ which is the major constituent phase after the initial milling of $6\text{LiBH}_4\text{-LaCl}_3$ [2] (see Fig. 1 Top) is no longer detected after ball-milling with LiH. Instead a broad and featureless bump is visible between 5 and 10° in 2θ and a modulation of the background at higher scattering angles. This indicates additional amorphous and/or nanocrystalline phases, possibly $\text{LaH}_{2+\delta}$. A similar nanostructured $\text{CeH}_{2+\delta}$ phase has been observed during thermal decomposition of $\text{Ce}(\text{BH}_4)_3$ [24]. The PXD pattern after desorption (400°C, 0.5 MPa) shows four major crystalline phases: LaB_6 , LiCl, $\text{LaH}_{2+\delta}$ and LiH, which are also present in the rehydrogenated sample. The two strongest peaks for the $\text{LaH}_{2+\delta}$ phase

are now clearly visible in the PXD pattern. The peak positions (lattice parameter) related to $\text{LaH}_{2+\delta}$ remain unchanged after rehydrogenation.

Figure 1

Fig. 2 shows the TG/DSC measurements of the $6\text{LiBH}_4\text{-LaCl}_3\text{-3LiH}$ composite at different stages, i.e. after ball-milling, desorption and rehydrogenation. The result for $6\text{LiBH}_4\text{-LaCl}_3$ after ball-milling is shown for comparison and has been discussed in [2]. The DSC curves have been divided into three major regions as indicated by vertical dashed lines in Fig. 2b and labelled (1) to (3). Below 300°C , the DSC trace of the as-milled $6\text{LiBH}_4\text{-LaCl}_3\text{-3LiH}$ composite shows endothermic signals at 105 and 285°C , caused by the orthorhombic to hexagonal structure transformation and melting of LiBH_4 , respectively. After milling with LiH, the endothermic events in region (2) have disappeared. They are caused by the partial decomposition of $\text{LiLa}(\text{BH}_4)_3\text{Cl}$ and the presence of a $\text{LiLa}(\text{BH}_4)_3\text{Cl-LiBH}_4$ composite [2]. Indeed, $\text{LiLa}(\text{BH}_4)_3\text{Cl}$ was found to be absent in the PXD pattern for $6\text{LiBH}_4\text{-LaCl}_3\text{-3LiH}$ after ball-milling (see Fig. 1). Finally, between 300 and 350°C a broad and intensive endothermic signal with a peak maximum at 320°C is visible that is accompanied by a loss of about 4.2 wt% H. The DSC curves after desorption against 0.5 MPa backpressure and rehydrogenation (10 MPa) show no presence of LiBH_4 . The TG-trace after rehydrogenation details a continuous small weight loss of about 0.8 wt% H between 150 and 330°C which indicates a very limited reversibility ($< 20\%$) under the present experimental condition. Since the lattice parameter of the $\text{LaH}_{2+\delta}$ phase in the PXD does not change after rehydrogenation, and no LiBH_4 is detected from the DSC curves after rehydrogenation, it follows that the small uptake of hydrogen for the $6\text{LiBH}_4\text{-LaCl}_3\text{-3LiH}$ composite must stem from some amorphous boron-containing phases.

Figure 2

6LiBH₄-ErCl₃-3LiH: The PXD pattern of as-milled 6LiBH₄-ErCl₃-3LiH in Fig. 3 shows the presence of three major crystalline phases: LiCl, LiBH₄ and LiH. Crystalline Er(BH₄)₃ which is the major constituent phase after the initial milling of 6LiBH₄-ErCl₃ (see Fig. 3 Top) is no longer detected after ball-milling with LiH. Instead the pattern exhibits a modulated background due to some amorphous and/or nanocrystalline components and broad shoulders on either side of the LiCl peaks, which could be attributed to the presence of ErH₃ and possibly ErH₂. However, ErH₂ is difficult to verify since it has almost identical lattice constant as LiCl, and/or could be hidden under the broad and modulated background. The sample desorbed against 0.5 MPa H₂ shows LiCl, ErB₄ and LiH as the major crystalline phases. The rehydrogenated sample also exhibits peaks corresponding to LiCl, ErB₄ and LiH, and in addition weak reflections caused by LiBH₄. The most intense peaks after rehydrogenation stem from ErH₃, which was not present in the desorbed sample.

Figure 3

Fig. 4 shows the TG/DSC measurements of the 6LiBH₄-ErCl₃-3LiH composite at different stages, i.e. after ball-milling, desorption and rehydrogenation. The result for 6LiBH₄-ErCl₃ after ball-milling is shown for comparison and has been discussed in [2]. The 6LiBH₄-ErCl₃ mixture shows the orthorhombic to hexagonal phase transition for LiBH₄ at 100 °C, and multiple endothermic events in the range 150 -200 °C, associated with the amorphization and partial decomposition of the parent borohydride phase, α-

$\text{Er}(\text{BH}_4)_3$, as previously reported [2, 11]. Finally, between 220 and 350 °C, a series of endothermic events is visible, with two relatively sharp ones around 240 and 290 °C, corresponding to the major decomposition of the parent borohydride phase and melting of LiBH_4 , respectively. Superimposed is a broad and featureless endothermic peak that stretches from 220 to 330 °C. For the $6\text{LiBH}_4\text{-ErCl}_3$ composite after ball-milling a total mass loss of about 5.2 wt% H is detected between RT and 400 °C. After the addition of LiH and a second milling procedure, the $6\text{LiBH}_4\text{-ErCl}_3\text{-3LiH}$ composite shows two major endothermic events (Fig. 4b) at about 105 and 285 °C, which are attributed to the presence of LiBH_4 . The thermal decomposition of $6\text{LiBH}_4\text{-ErCl}_3\text{-3LiH}$ starts at about 300 °C, and is accompanied by a mass loss of about 3 wt% H. The TG/DSC trace of the dehydrogenated sample against 0.5 MPa backpressure is flat and exhibits no signals from LiBH_4 .

Figure 4

However, the DSC curve of the rehydrogenated $6\text{LiBH}_4\text{-ErCl}_3\text{-3LiH}$ sample contains two endothermic signals clearly caused by the presence of LiBH_4 , and a broad endothermic signal similar to the one observed for the as-milled composite. The rehydrogenated sample exhibits an accumulated mass loss of about 2.4 wt% H up to 400 °C, and thus shows an excellent reversibility (~80%) after desorption against 0.5 MPa backpressure. With desorption against vacuum the mass loss for the rehydrogenated sample is ~2.0 wt% H up to 400 °C (not shown) and thus reaches ~66% reversibility.

These findings are in contrast to the composite containing lanthanum (see above) where only very limited reversibility of ~19% was found. In light of the PXD and TG/DSC results it can be concluded that the improved capacity on rehydrogenation compared to the lanthanum containing composite is caused

by the formation of ErH_3 and the rehydrogenation of LiBH_4 . This is a remarkable result since the rehydrogenation of pure LiBH_4 requires usually much harsher conditions, $>400\text{ }^\circ\text{C}$ and $>10\text{ MPa H}_2$ [25, 26].

Discussion

The as-milled $6\text{LiBH}_4\text{-RECl}_3$ samples ($\text{RE} = \text{La, Er}$) contain $\text{LiLa}(\text{BH}_4)_3\text{Cl}$ and $\text{Er}(\text{BH}_4)_3$ in product mixtures with excess LiBH_4 and LiCl according to previous publication [2]. These composites release hydrogen at around $210\text{ }^\circ\text{C}$ (La) and $180\text{ }^\circ\text{C}$ (Er), respectively, and yield about 5.5 wt% H (La) and 5.2 wt% H (Er) in total up to $400\text{ }^\circ\text{C}$. The thermal decomposition of both $6\text{LiBH}_4\text{-RECl}_3$ composites follows a complicated multistep process that involves several intermediate phases until the final products, mainly LaB_6 , ErB_4 and traces of $\text{REH}_{2+\delta}$ are formed [2]. The formation of $\text{REH}_{2+\delta}$ species through decomposition of the parent borohydride phase destabilizes the excess LiBH_4 and leads to a gas release at significantly lower temperatures ($\sim 200\text{ }^\circ\text{C}$) compared to pure ball-milled LiBH_4 ($\sim 400\text{ }^\circ\text{C}$) [13]. A similar destabilization effect has also been observed in other composites containing LiBH_4 and metal hydrides, e.g. $6\text{LiBH}_4\text{-CaH}_2$ [27, 28], $6\text{LiBH}_4\text{-CeH}_2$ [24, 27, 28] and $4\text{LiBH}_4\text{-YH}_3$ [27].

$6\text{LiBH}_4\text{-RECl}_3\text{-3LiH}$ ($\text{RE} = \text{La, Er}$) that are formed after the additional milling procedure with LiH show a simplified thermal decomposition as compared to composites without LiH (see Figs. 2 and 4). Although desorption starts at higher temperatures ($\sim 300\text{ }^\circ\text{C}$), both systems still liberate 4 wt% H (La) and 3 wt% H (Er) respectively, in a narrow temperature interval between 300 and $350\text{ }^\circ\text{C}$. The kinetics of hydrogen desorption appear to be enhanced as compared to $6\text{LiBH}_4\text{-RECl}_3$. For $6\text{LiBH}_4\text{-LaCl}_3\text{-3LiH}$, 4 wt% H are desorbed within a temperature range of $50\text{ }^\circ\text{C}$, whereas the same amount of gas is released within $100\text{ }^\circ\text{C}$ in the $6\text{LiBH}_4\text{-LaCl}_3$ composite. Since all TG/DSC experiments were carried out with the same heating rate, it follows that gas desorption is almost twice as fast for $6\text{LiBH}_4\text{-LaCl}_3\text{-3LiH}$. The effect is less

pronounced for 6LiBH₄-ErCl₃-3LiH, yet 3 wt% H are released within an interval of 75 °C, whereas the same amount of gas is desorbed within 100 °C from the 6LiBH₄-ErCl₃ composite.

Gennari et al. [13] recently investigated the thermal behavior and reversibility of 6LiBH₄-RECl₃ composites (RE=Ce, Gd) with and without addition of LiH. The authors state that the presence of LiH in the second milling step leads to the formation of CeH_{2+δ}. In the current study for 6LiBH₄-LaCl₃-3LiH, peaks for nanoscale LaH_{2+δ} are visible after ball-milling from the PXD pattern in Fig 1. This finding combined with the TG/DSC result in Fig. 2 indicates the disappearance of LiLa(BH₄)₃Cl after ball-milling with LiH, and strongly suggests that LaH_{2+δ} is formed via the interaction of LiH with the parent borohydride phase LiLa(BH₄)₃Cl:

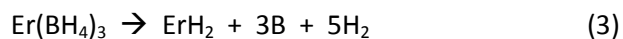
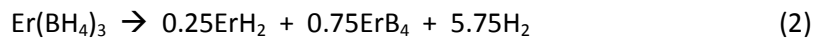


The thermal decomposition of 6LiBH₄-LaCl₃-3LiH yields 4.2 wt% H during the first cycle and 0.8 wt% H during the second cycle after rehydrogenation. The system shows only a very limited capacity for rehydrogenation (~19%) under these experimental conditions. In a previous report on 6LiBH₄-LaCl₃ mixtures desorbed against vacuum we also observed only 18% recovery at 300 °C and 36% at 415 °C [2]. Neither the addition of LiH nor the application of backpressure in the present study seems to have a beneficial effect on the reversibility in the lanthanum containing composites. This is a surprising result since backpressure is expected to promote the formation of LaB₆ over amorphous boron and the addition of LiH should enhance the reversibility of LaB₆. It is at present not clear why the lanthanum containing composite shows such a poor reversibility whereas the 6LiBH₄-CeCl₃-3LiH system investigated

by Gennari et al. (note both parent RE-borohydrides are isostructural) is able to recover between 45 and 80% of its initial hydrogen capacity [13].

In this paper we have compared for the first time the thermal properties of erbium-based $6\text{LiBH}_4\text{-RECl}_3$ composites with and without addition of LiH. For $6\text{LiBH}_4\text{-ErCl}_3$, we observe a mass loss of about 5.2 wt% H in the temperature region between RT and 400 °C. The mixture releases 1.4 wt% H after rehydrogenation (415 °C, 10 MPa) during the second dehydrogenation cycle, which corresponds to ~25% reversibility [2]. In comparison, Gennari et al. have reported a gas release of about 5 wt% H from a gadolinium-based $6\text{LiBH}_4\text{-GdCl}_3$ composite during the first dehydrogenation cycle and 2.0 and 1.7 wt% H gas evolution during the second dehydrogenation cycle under vacuum and against 0.5 MPa backpressure, respectively [13]. Since the parent borohydrides $\text{Er}(\text{BH}_4)_3$ and $\text{Gd}(\text{BH}_4)_3$ in both mixtures are isostructural [1, 2], and similar decomposition products (ErB_4 vs. GdB_4) are formed, we can expect similar behavior during decomposition.

In contrast, as-milled $6\text{LiBH}_4\text{-ErCl}_3\text{-3LiH}$ desorbs only about 3.0 wt% H up to 350 °C. Samples decomposed against vacuum and backpressure release 2.0 wt% H and 2.4 wt% H after rehydrogenation, respectively. The $6\text{LiBH}_4\text{-ErCl}_3\text{-3LiH}$ composite shows therefore a reversibility of 66% under vacuum and 80% against 0.5 MPa backpressure. The decomposition of the parent $\text{Er}(\text{BH}_4)_3$ phase in $6\text{LiBH}_4\text{-ErCl}_3\text{-3LiH}$ is proposed to follow two pathways according to (2) and (3):



The experimental conditions will have a strong influence on the relative ratio between these two alternative pathways, and desorption under backpressure is expected to favor the formation of ErB_4 over elemental boron. A similar effect has been observed for the combination of LiBH_4 with reactive additives such as MgH_2 [29-31], CaH_2 [28] and Al [32, 33]. Indeed analysis of the relative intensities for ErB_4 and LiCl in the PXD patterns show a slight intensity increase for ErB_4 after desorption against 0.5 MPa hydrogen as compared to vacuum. $6\text{LiBH}_4\text{-ErCl}_3\text{-3LiH}$ shows good reversibility ($\sim 66\%$) for samples desorbed under vacuum and even higher reversibility ($\sim 80\%$) after dehydrogenation under hydrogen backpressure. Hydrogen uptake of the mixture could be realized through the interaction between the decomposition product ErB_4 , LiH and hydrogen. This will result in the formation of $\text{ErH}_{2+\delta}$ and LiBH_4 . This assumption seems plausible and is furthermore supported by experimental observations, in particular the reappearance of LiBH_4 in the DSC-curve (Fig. 4b) and peaks belonging to ErH_3 (cubic, $a=5.27 \text{ \AA}$) in the PXD pattern (Fig. 3) for the rehydrogenated samples.

For $6\text{LiBH}_4\text{-GdCl}_3\text{-3LiH}$ composites, Gennari et al.[13] have reported a slightly higher gas release under vacuum than against backpressure (5.0 % vs. 4.9 %) during the first dehydrogenation cycle and a slightly larger difference during the second dehydrogenation cycle (2.0 % vs 1.7 %). This is in contrast to what we observe for $6\text{LiBH}_4\text{-ErCl}_3\text{-3LiH}$, where the sample desorbed against backpressure shows a larger gas release (2.4% vs. 2.0%) after rehydrogenation. These findings could be caused by differences in experimental conditions such as temperature, pressure and time during the cycling experiments, sample morphology and/or final composition in the $6\text{LiBH}_4\text{-RECl}_3\text{-3LiH}$ composites after ball-milling.

Conclusion

The mechanochemical reaction between LiBH_4 , $\text{LaCl}_3 / \text{ErCl}_3$ and LiH in a molar ratio of 6:1:3 has led to the formation of composite mixtures that release between 3 wt% H (Er) and 4.2 wt% H (La) above 300 °C. In both composites RE-hydride species, $\text{REH}_{2+\delta}$, are formed during heating which destabilize excess LiBH_4 and lower its desorption temperature by about 100 °C. The kinetics of hydrogen release is significantly increased compared to $6\text{LiBH}_4\text{-RECl}_3$ composites without LiH . The lanthanum-containing mixture shows only a limited rehydrogenation capacity of <20% (340 °C, 10 MPa). The erbium-containing samples regain 66% of their original hydrogen storage capacity after rehydrogenation when desorbed against vacuum. This value increases up to 80% when desorbed against 0.5 MPa backpressure.

Acknowledgements

The Research Council of Norway is acknowledged for financial support through the SYNKNØYT program. We acknowledge the skillful assistance from the staff of SNBL at ESRF, Grenoble in France.

Figure Captions

Figure 1: SR-PXD pattern ($\lambda = 0.50513 \text{ \AA}$) of $6\text{LiBH}_4\text{-LaCl}_3$ mixture obtained after ball-milling (Top) and $6\text{LiBH}_4\text{-LaCl}_3\text{-3LiH}$ after ball-milling, desorption against 0.5 MPa backpressure and rehydrogenation ($340 \text{ }^\circ\text{C}$, 10 MPa).

Figure 2: (A) TG-trace of $6\text{LiBH}_4\text{-LaCl}_3$ composite obtained after ball-milling and $6\text{LiBH}_4\text{-LaCl}_3\text{-3LiH}$ after ball-milling, desorption against 0.5 MPa backpressure and rehydrogenation ($340 \text{ }^\circ\text{C}$, 10 MPa). (B) DSC trace of the composite mixtures described under (A) in the temperature region between RT and $400 \text{ }^\circ\text{C}$.

Figure 3: SR-PXD pattern ($\lambda = 0.50513 \text{ \AA}$) of $6\text{LiBH}_4\text{-ErCl}_3$ mixture obtained after ball-milling (Top) and $6\text{LiBH}_4\text{-ErCl}_3\text{-3LiH}$ after ball-milling, desorption against 0.5 MPa backpressure and rehydrogenation ($340 \text{ }^\circ\text{C}$, 10 MPa).

Figure 4: (A) TG-trace of $6\text{LiBH}_4\text{-ErCl}_3$ composite obtained after ball-milling and $6\text{LiBH}_4\text{-ErCl}_3\text{-3LiH}$ composite mixtures after ball-milling, desorption against 0.5 MPa backpressure and rehydrogenation ($340 \text{ }^\circ\text{C}$, 10 MPa). (B) DSC trace of the composite mixtures described under (A) in the temperature region between RT and $400 \text{ }^\circ\text{C}$.

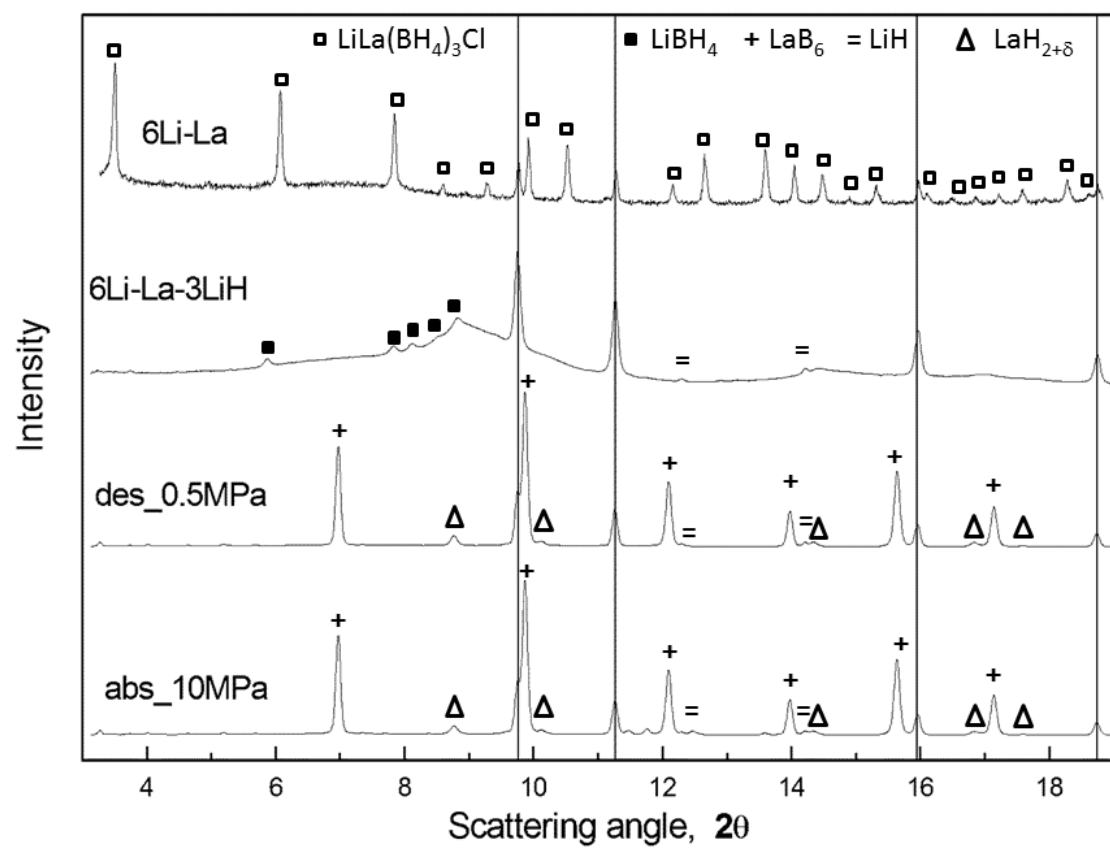


Figure 1:

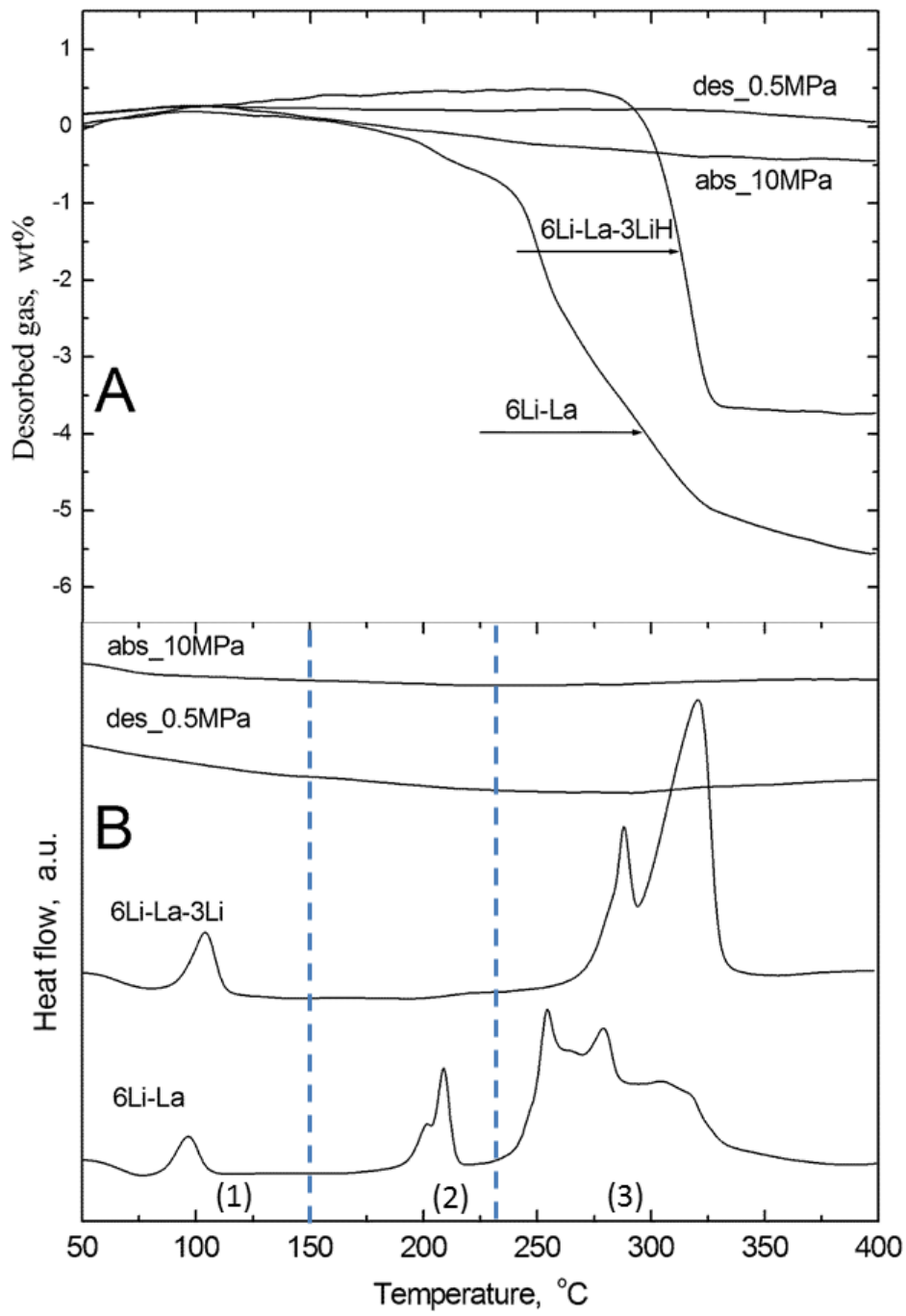


Figure 2:

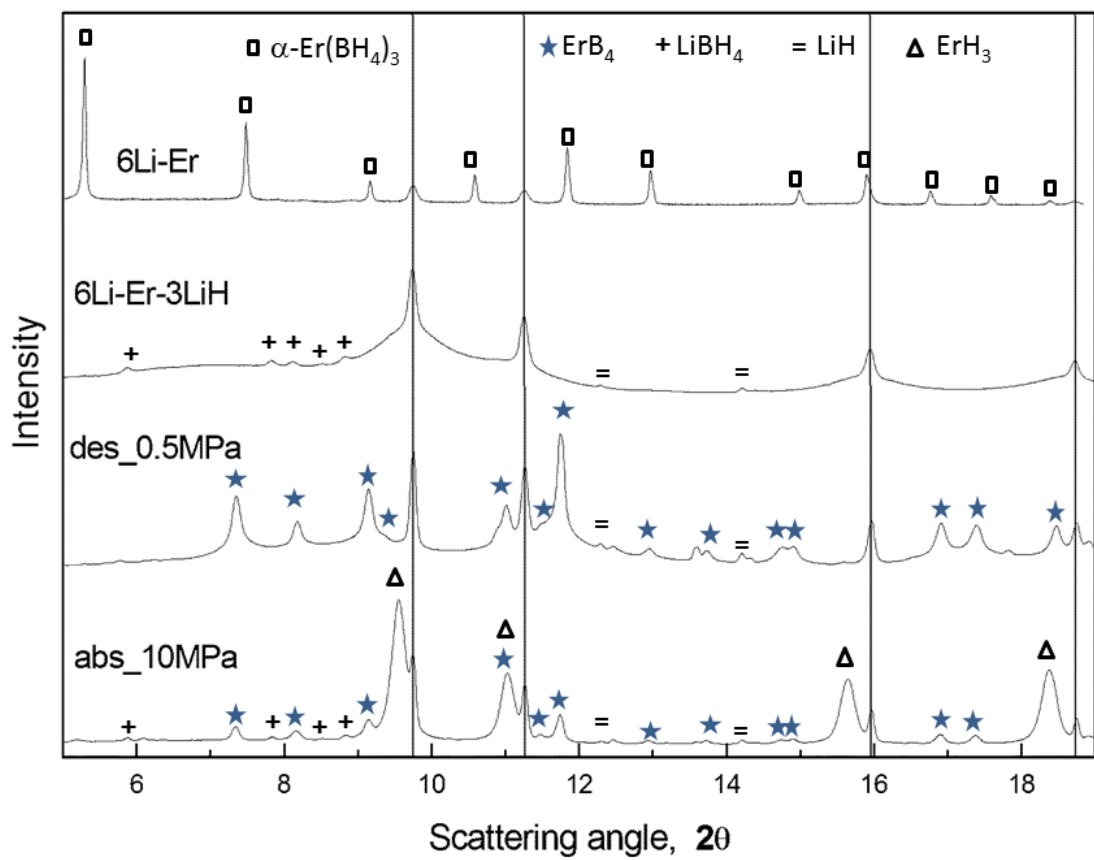


Figure 3:

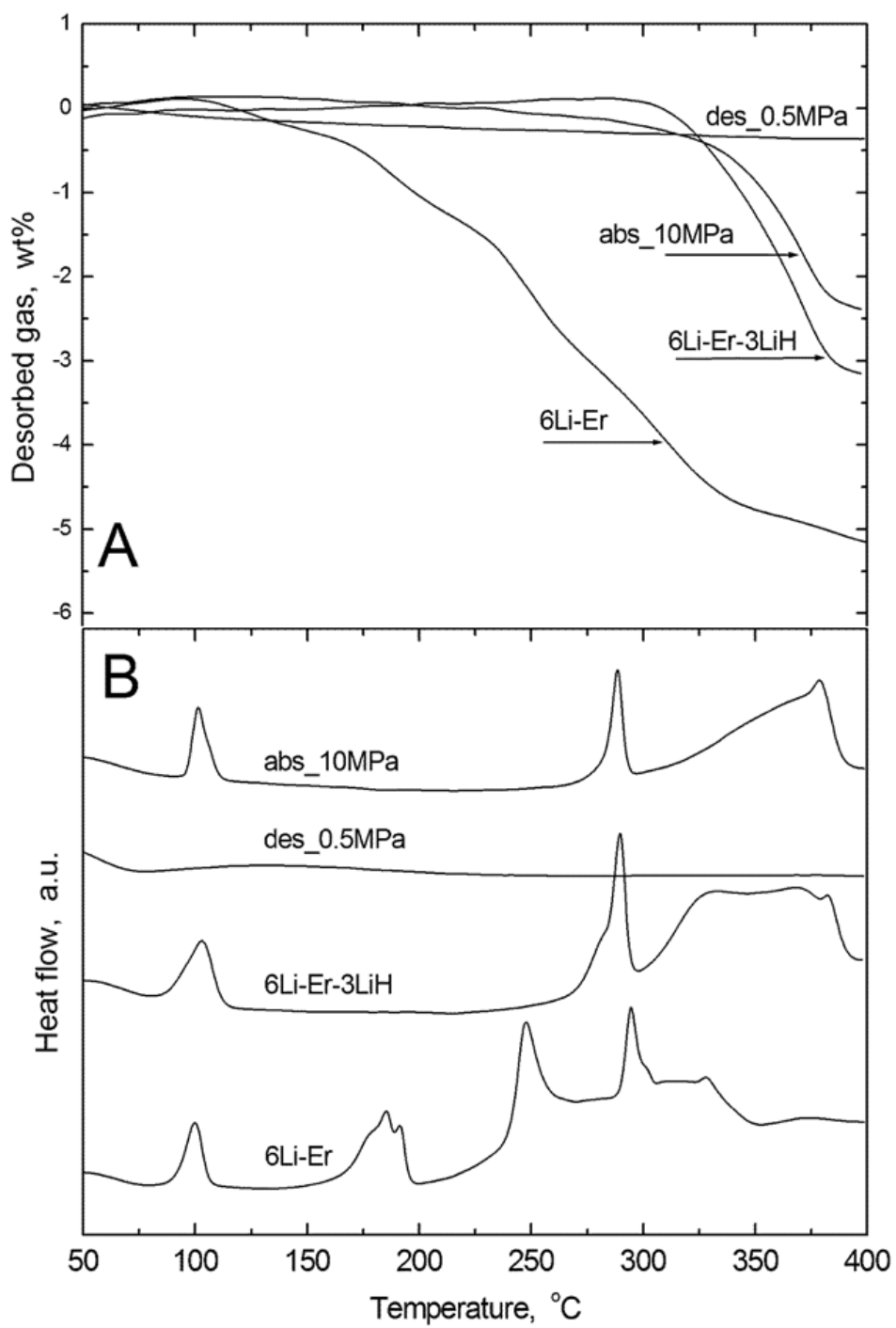


Figure 4:

References

- [1] T. Sato, K. Miwa, Y. Nakamori, K. Ohoyama, H.W. Li, T. Noritake, M. Aoki, S.I. Towata, S.I. Orimo, Experimental and computational studies on solvent-free rare-earth metal borohydrides $R(\text{BH}_4)_3$ ($R = \text{Y}$, Dy , and Gd), *Physical Review B* 77 (2008).
- [2] J.E. Olsen, C. Frommen, T.R. Jensen, M.D. Riktor, M.H. Sørby, B.C. Hauback, Structure and thermal properties of composites with RE-borohydrides ($\text{RE} = \text{La}$, Ce , Pr , Nd , Sm , Eu , Gd , Tb , Er , Yb or Lu) and LiBH_4 , *RSC Advances* 4 (2014) 1570-1582.
- [3] J.E. Olsen, C. Frommen, M.H. Sørby, B.C. Hauback, Crystal structures and properties of solvent-free $\text{LiYb}(\text{BH}_4)_{4-x}\text{Cl}_x$, $\text{Yb}(\text{BH}_4)_3$ and $\text{Yb}(\text{BH}_4)_{2-x}\text{Cl}_x$, *RSC Advances* 3 (2013) 10764-10774.
- [4] T. Jaron, W. Grochala, $\text{Y}(\text{BH}_4)_3$ -an old-new ternary hydrogen store aka learning from a multitude of failures, *Dalton Transactions* 39 (2010) 160-166.
- [5] C. Frommen, N. Aliouane, S. Deledda, J.E. Fonnelløp, H. Grove, K. Lieutenant, I. Llamas-Jansa, S. Sartori, M.H. Sørby, B.C. Hauback, Crystal structure, polymorphism, and thermal properties of yttrium borohydride $\text{Y}(\text{BH}_4)_3$, *Journal of Alloys and Compounds* 496 (2010) 710-716.
- [6] C. Frommen, M.H. Sørby, P. Ravindran, P. Vajeeston, H. Fjellvåg, B.C. Hauback, Synthesis, Crystal Structure, and Thermal Properties of the First Mixed-Metal and Anion-Substituted Rare Earth Borohydride $\text{LiCe}(\text{BH}_4)_3\text{Cl}$, *Journal of Physical Chemistry C* 115 (2011) 23591-23602.
- [7] D.B. Ravnsbæk, Y. Filinchuk, R. Cerny, M.B. Ley, D. Haase, H.J. Jakobsen, J. Skibsted, T.R. Jensen, Thermal Polymorphism and Decomposition of $\text{Y}(\text{BH}_4)_3$, *Inorganic Chemistry* 49 (2010) 3801-3809.
- [8] M.B. Ley, L.H. Jepsen, Y.S. Lee, Y.W. Cho, J.M.B. von Colbe, M. Dornheim, M. Rokni, J.O. Jensen, M. Sloth, Y. Filinchuk, J.E. Jorgensen, F. Besenbacher, T.R. Jensen, Complex hydrides for hydrogen storage - new perspectives, *Materials Today* 17 (2014) 122-128.
- [9] Y.G. Yan, H.W. Li, T. Sato, N. Umeda, K. Miwa, S. Towata, S.I. Orimo, Dehydrogenating and rehydrogenating properties of yttrium borohydride $\text{Y}(\text{BH}_4)_3$ prepared by liquid-phase synthesis, *International Journal of Hydrogen Energy* 34 (2009) 5732-5736.
- [10] T. Jaron, W. Kozminkia, W. Grochala, Phase transition induced improvement in H_2 desorption kinetics: the case of the high-temperature form of $\text{Y}(\text{BH}_4)_3$, *Physical Chemistry Chemical Physics* 13 (2011) 8847-8851.
- [11] F.C. Gennari, Mechanochemical synthesis of erbium borohydride: Polymorphism, thermal decomposition and hydrogen storage, *Journal of Alloys and Compounds* 581 (2013) 192-195.
- [12] F.C. Gennari, M.R. Esquivel, Synthesis and dehydrogenating process of crystalline $\text{Ce}(\text{BH}_4)_3$, *Journal of Alloys and Compounds* 485 (2009) L47-L51.
- [13] F.C. Gennari, L.F. Albanesi, J.A. Puzkiel, P.A. Larochette, Reversible hydrogen storage from $6\text{LiBH}_4 - \text{MCl}_3$ ($\text{M} = \text{Ce}$, Gd) composites by in-situ formation of MH_2 , *International Journal of Hydrogen Energy* 36 (2011) 563-570.
- [14] H.W. Li, Y.G. Yan, S.I. Orimo, A. Züttel, C.M. Jensen, Recent Progress in Metal Borohydrides for Hydrogen Storage, *Energies* 4 (2011) 185-214.
- [15] B.J. Zhang, B.H. Liu, Z.P. Li, Destabilization of LiBH_4 by $(\text{Ce}, \text{La})(\text{Cl}, \text{F})_3$ for hydrogen storage, *Journal of Alloys and Compounds* 509 (2011) 751-757.
- [16] M.B. Ley, D.B. Ravnsbæk, Y. Filinchuk, Y.S. Lee, R. Janot, Y.W. Cho, J. Skibsted, T.R. Jensen, $\text{LiCe}(\text{BH}_4)_3\text{Cl}$, a New Lithium-Ion Conductor and Hydrogen Storage Material with Isolated Tetranuclear Anionic Clusters, *Chemistry of Materials* 24 (2012) 1654-1663.

- [17] M.B. Ley, S. Boulineau, R. Janot, Y. Filinchuk, T.R. Jensen, New Li Ion Conductors and Solid State Hydrogen Storage Materials: $\text{LiM}(\text{BH}_4)_3\text{Cl}$, $\text{M} = \text{La, Gd}$, *Journal of Physical Chemistry C* 116 (2012) 21267-21276.
- [18] A.V. Skripov, A.V. Soloninin, M.B. Ley, T.R. Jensen, Y. Filinchuk, Nuclear Magnetic Resonance Studies of BH_4 Reorientations and Li Diffusion in $\text{LiLa}(\text{BH}_4)_3\text{Cl}$, *Journal of Physical Chemistry C* 117 (2013) 14965-14972.
- [19] H. Hagemann, R. Cerny, Synthetic approaches to inorganic borohydrides, *Dalton Transactions* 39 (2010) 6006-6012.
- [20] K. Park, H.S. Lee, A. Remhof, Y.S. Lee, Y.G. Yan, M.Y. Kim, S.J. Kim, A. Züttel, Y.W. Cho, Thermal properties of $\text{Y}(\text{BH}_4)_3$ synthesized via two different methods, *International Journal of Hydrogen Energy* 38 (2013) 9263-9270.
- [21] O. Friedrichs, A. Remhof, A. Borgschulte, F. Buchter, S.I. Orimo, A. Züttel, Breaking the passivation-the road to a solvent free borohydride synthesis, *Physical Chemistry Chemical Physics* 12 (2010) 10919-10922.
- [22] H. Hagemann, M. Longhini, J.W. Kaminski, T.A. Wesolowski, R. Cerny, N. Penin, M.H. Sørby, B.C. Hauback, G. Severa, C.M. Jensen, $\text{LiSc}(\text{BH}_4)_4$: A novel salt of Li^+ and discrete $\text{Sc}(\text{BH}_4)_4^-$ complex anions, *Journal of Physical Chemistry A* 112 (2008) 7551-7555.
- [23] E.M. Fedneva, V.I. Alpatova, V.I. Mikheeva, *Termicheskaya Ustoichivost Borogidrida Litiya*, *Zhurnal Neorganicheskoi Khimii* 9 (1964) 1519-1520.
- [24] F.C. Gennari, Destabilization of LiBH_4 by MH_2 ($\text{M} = \text{Ce, La}$) for hydrogen storage: Nanostructural effects on the hydrogen sorption kinetics, *International Journal of Hydrogen Energy* 36 (2011) 15231-15238.
- [25] P. Mauron, F. Buchter, O. Friedrichs, A. Remhof, M. Biemann, C.N. Zwicky, A. Züttel, Stability and reversibility of LiBH_4 , *Journal of Physical Chemistry B* 112 (2008) 906-910.
- [26] S. Orimo, Y. Nakamori, G. Kitahara, K. Miwa, N. Ohba, S. Towata, A. Züttel, Dehydriding and rehydriding reactions of LiBH_4 , *Journal of Alloys and Compounds* 404 (2005) 427-430.
- [27] J.H. Shim, J.H. Lim, S.U. Rather, Y.S. Lee, D. Reed, Y. Kim, D. Book, Y.W. Cho, Effect of Hydrogen Back Pressure on Dehydrogenation Behavior of LiBH_4 -Based Reactive Hydride Composites, *Journal of Physical Chemistry Letters* 1 (2010) 59-63.
- [28] S.A. Jin, Y.S. Lee, J.H. Shim, Y.W. Cho, Reversible hydrogen storage in $\text{LiBH}_4\text{-MH}_2$ ($\text{M} = \text{Ce, Ca}$) composites, *Journal of Physical Chemistry C* 112 (2008) 9520-9524.
- [29] J.J. Vajo, S.L. Skeith, F. Mertens, Reversible storage of hydrogen in destabilized LiBH_4 , *Journal of Physical Chemistry B* 109 (2005) 3719-3722.
- [30] J.J. Vajo, T.T. Salguero, A.E. Gross, S.L. Skeith, G.L. Olson, Thermodynamic destabilization and reaction kinetics in light metal hydride systems, *Journal of Alloys and Compounds* 446 (2007) 409-414.
- [31] U. Bösenberg, S. Doppiu, L. Mosegaard, G. Barkhordarian, N. Eigen, A. Borgschulte, T.R. Jensen, Y. Cerenius, O. Gutfleisch, T. Klassen, M. Dornheim, R. Bormann, Hydrogen sorption properties of $\text{MgH}_2\text{-LiBH}_4$ composites, *Acta Materialia* 55 (2007) 3951-3958.
- [32] S.A. Jin, J.H. Shim, Y.W. Cho, K.W. Yi, O. Zabara, M. Fichtner, Reversible hydrogen storage in $\text{LiBH}_4\text{-Al-LiH}$ composite powder, *Scripta Materialia* 58 (2008) 963-965.
- [33] Y. Zhang, Q.F. Tian, J. Zhang, S.S. Liu, L.X. Sun, The Dehydrogenation Reactions and Kinetics of $2\text{LiBH}_4\text{-Al}$ Composite, *Journal of Physical Chemistry C* 113 (2009) 18424-18430.